

## Muon spin relaxation study of $\text{LaTiO}_3$ and $\text{YTiO}_3$

P. J. Baker<sup>1</sup>, T. Lancaster<sup>1</sup>, S. J. Blundell<sup>1</sup>, W. Hayes<sup>1</sup>,  
F. L. Pratt<sup>2</sup>, M. Itoh<sup>3</sup>, S. Kuroiwa<sup>4</sup> and J. Akimitsu<sup>4</sup>

<sup>1</sup> Department of Physics, Oxford University, Parks Road, Oxford OX1 3PU, United Kingdom

<sup>2</sup> ISIS Muon Facility, Rutherford Appleton Laboratory, Harwell Science and Innovation Campus, Didcot, OX11 0QX, United Kingdom

<sup>3</sup> Department of Physics, Nagoya University, Nagoya 464-8602, Japan

<sup>4</sup> Department of Physics, Aoyama Gakuin University, Sagamihara, Kanagawa 229-8558, Japan

E-mail: p.baker1@physics.ox.ac.uk

**Abstract.** We report muon spin relaxation ( $\mu\text{SR}$ ) measurements on two  $\text{Ti}^{3+}$  containing perovskites,  $\text{LaTiO}_3$  and  $\text{YTiO}_3$ , which display long range magnetic order at low temperature. For both materials, oscillations in the time-dependence of the muon polarization are observed which are consistent with three-dimensional magnetic order. From our data we identify two magnetically inequivalent muon stopping sites. The  $\mu\text{SR}$  results are compared with the magnetic structures of these compounds previously derived from neutron diffraction and  $\mu\text{SR}$  studies on structurally similar compounds.

PACS numbers: 76.75.+i, 75.25.+z, 75.50.Cc, 75.50.Ee

Submitted to: *JPCM*

## 1. Introduction

Despite their structural simplicity (exemplified in Figure 1) perovskite compounds of the form  $\text{ABX}_3$  show a wide variety of physical properties, particularly when the simple cubic structure is distorted [1]. Changing the ionic radius of the ion on the A site allows the distortion to be controlled and, through this, the physics of these materials can be tuned [2]. An example of two similar compounds where a small change in the ionic radius causes a significant change in the physical properties is the pair  $\text{LaTiO}_3$  and  $\text{YTiO}_3$ .

These two compounds are Mott-Hubbard insulators but retain the orbital degree of freedom in the  $t_{2g}$  state [3] and show a strong coupling between spin and orbital degrees of freedom [4]. Orbital degeneracy, which can lead to phenomena such as colossal magnetoresistance or unconventional superconductivity [5], is present in isolated Ti  $t_{2g}$  ions, but is lifted in these compounds [4]. The size of the  $\text{A}^{3+}$  ion provides one means of tuning the properties of these titanates [4], affecting the Ti-O-Ti bond angles and exchange interactions. This is evident in the difference between the low temperature magnetic structures of these two compounds, observed using neutron diffraction [6, 7, 8].  $\text{LaTiO}_3$  is a G-type antiferromagnet with the Ti moments aligned along the  $a$ -axis [6, 7] below  $T_N$ . The precise value of  $T_N$  is very sensitive to the oxygen stoichiometry and reports vary between 120 and  $\sim 150$  K [9].  $\text{YTiO}_3$  orders ferromagnetically [8] with the spins aligned along the  $c$ -axis at  $T_C = 27$  K; however, there is a G-type antiferromagnetic component along  $a$ , and an A-type component along  $b$  (see figure 1).

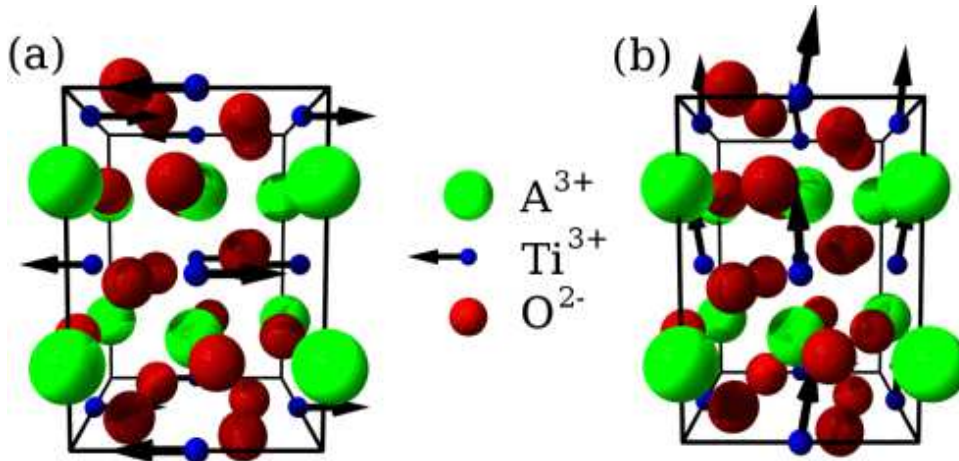


**Figure 1.** (a)  $\text{LaTiO}_3$  and (b)  $\text{YTiO}_3$ , showing the magnetic structures previously proposed. Structural parameters were taken from Refs. [7] & [10], and magnetic structures from Refs. [7] & [8].

Evidence of orbital excitations due to fluctuations of orbital-exchange bonds has been found in  $\text{LaTiO}_3$  and  $\text{YTiO}_3$  using Raman scattering, and these excitations are remarkably similar to the exchange-bond fluctuations which give rise to magnetic Raman scattering in cuprates [9]. A broad range of measurements have demonstrated

the underlying orbital ordering in both compounds [2, 7, 11, 12, 13, 14], strongly excluding the orbital liquid picture hypothesized for  $\text{LaTiO}_3$  [15] and agreeing with the reduced orbital moment found in X-ray and NMR measurements on  $\text{LaTiO}_3$  [6, 16]. It has been shown [17] that the  $\text{Y}_{1-x}\text{La}_x\text{TiO}_3$  system is an itinerant-electron antiferromagnet with no orbital ordering for  $x > 0.7$  and that an intermediate phase exists for  $0.3 < x < 0.7$ , with orbital-order fluctuations and ferromagnetic interactions that reduce  $T_N$ . For  $x < 0.3$  the system shows orbital ordering and a ferromagnetic transition and it was suggested that even at  $x = 0$  the volume of the orbitally ordered region does not encompass the whole sample.

Theoretical work on these compounds has focused around the mechanism that selects the ground state from the possible spin and orbital configurations. Models considering the orbitals as quasi-static entities [3, 7, 18, 19, 20] satisfactorily predict the orbital occupation and magnetic ordering. Nevertheless, there remain aspects of the experimental observations [6, 8, 9] that cannot be successfully described without including the quantum fluctuations of the orbitals [15, 21, 22], particularly with regard to the Raman scattering results. With quasi-static orbital occupations, excitations are in the form of well-defined crystal field excitations, whereas if fluctuations are significant, the excitations are collective modes, and it is the latter which are observed by Raman scattering experiments [9]. Predicting the magnetic properties of these compounds based on their structures (i.e. the tuning provided by the  $A$ -site cation radius) and their observed orbital physics has proved challenging, particularly for  $\text{LaTiO}_3$  [3]. In this context, additional detailed characterisation of the magnetic properties of both compounds is worthwhile, in the hope of providing information to further constrain the theoretical models.

In this paper we describe the results of a muon-spin relaxation ( $\mu\text{SR}$ ) investigation into the magnetic properties of  $\text{LaTiO}_3$  and  $\text{YTiO}_3$ . The methods of synthesis and the experimental details common to both compounds are explained in section 2. The results of the  $\mu\text{SR}$  experiments are presented in sections 3 and 4. Dipole field calculations for magnetic structures previously deduced by neutron diffraction are compared to the  $\mu\text{SR}$  results in section 5. The results are discussed and conclusions are drawn in section 6.

## 2. Experimental

The  $\text{LaTiO}_3$  sample was synthesized by arc melting appropriate mixtures of  $\text{La}_2\text{O}_3$ ,  $\text{TiO}_2$ , and  $\text{Ti}$  in an argon atmosphere [23]. The properties of  $\text{LaTiO}_3$  are strongly dependent on the oxygen stoichiometry (see, for examples, Refs. [9, 17]). To produce a sample as close to the correct stoichiometry as possible, several samples were prepared and one with  $T_N = 135$  K, determined by magnetic measurements, was chosen. The  $\text{YTiO}_3$  was prepared similarly, using  $\text{Y}_2\text{O}_3$ , and was determined to be  $\text{YTiO}_{3+\delta}$  with  $\delta \leq 0.05$ ,  $T_C = 27$  K, and a saturation magnetic moment of  $0.84\mu_B/\text{Ti}$  [13].

Our  $\mu\text{SR}$  experiments on both samples were carried out using the GPS instrument at the Paul Scherrer Institute, in zero applied magnetic field (ZF). In a  $\mu\text{SR}$  experiment [24] spin polarized positive muons are implanted into the sample, generally stopping at an interstitial position within the crystal structure, without significant loss of polarization. The polarization,  $P_z(t)$ , of the muon subsequently depends on the magnetic environment of the stopping site and can be measured using the asymmetric decay of the muon, with around 20 million muon decays recorded for each temperature point considered. The emitted positron is detected in scintillation

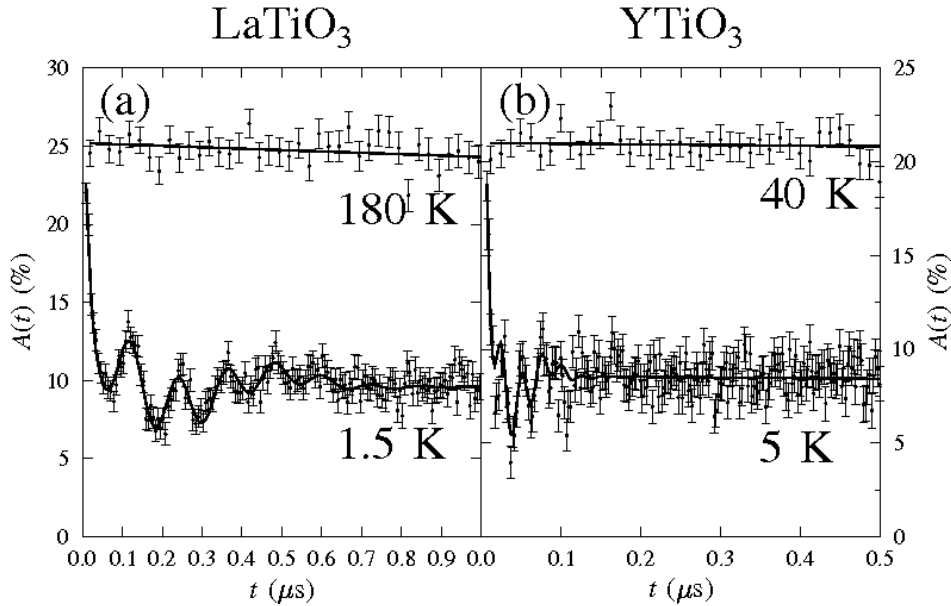


**Figure 2.** Examples of the raw  $\mu\text{SR}$  data recorded for (a)  $\text{LaTiO}_3$  and (b)  $\text{YTiO}_3$ . For both compounds, the precession is clearly evident in the low temperature data and absent in the high temperature data. For the low-temperature datasets the lines plotted are fits of the data to Equation 1, and for the high-temperature datasets the lines are fits to an exponential relaxation, as discussed in the text.

counters around the sample position [24]. The asymmetry of the positron counts is  $A(t) = (A(0) - A_{\text{bg}})P_z(t) + A_{\text{bg}}$ , with  $A(0) \sim 25\%$  (see Figure 2) and  $A_{\text{bg}}$  a small contribution to the signal due to muons stopping outside the sample. The polycrystalline samples were wrapped in silver foil packets and mounted on a silver backing plate, since the small nuclear magnetic moment of silver minimizes the relaxing contribution of the sample mount to  $A_{\text{bg}}$ . Examples of the measured asymmetry spectra in both compounds are presented in Figure 2. At low temperature, precession signals are seen in both compounds, indicative of long-range magnetic order, with two precession frequencies (see Figures 3 and 4) indicating two magnetically inequivalent muon sites. Above their respective transition temperatures the data for both compounds shows exponential relaxation characteristic of a paramagnetic phase.

After the initial positron decay asymmetry,  $A(0)$ , and the background,  $A_{\text{bg}}$ , had been determined, the following equation was used to analyse the asymmetry data below the magnetic ordering temperature in each compound:

$$P_z(t) = P_{\text{f}}e^{-\lambda t} + P_{\text{r}}e^{-\sigma_{\text{r}}^2 t^2} + P_{\text{osc}}e^{-\sigma_{\text{osc}}^2 t^2} [\cos(2\pi\nu_1 t) + \cos(2\pi\nu_2 t)]. \quad (1)$$

The components  $P_{\text{f}}$ ,  $P_{\text{r}}$ , and  $P_{\text{osc}}$  are all independent of temperature and are in the ratio  $(P_{\text{f}} + P_{\text{r}})/P_{\text{osc}} \simeq 2$  expected from polycrystalline averaging. The exponentially relaxing component  $P_{\text{f}}$  can be attributed to fluctuating fields parallel to the direction

of the implanted muon spin, and the relaxation rate,  $\lambda$  was found to be almost independent of temperature. A Gaussian relaxing component,  $P_r$ , describes the rapid drop in the asymmetry at short times, due to large magnetic fields at a muon stopping site, and the  $P_{\text{osc}}$  term describes the two-frequency oscillating component of the signal due to coherent local magnetic fields at two magnetically inequivalent muon stopping sites (we take  $\nu_1 > \nu_2$ ). The data were fitted throughout the ordered temperature range while fixing the ratio  $\nu_2/\nu_1$  to the value obtained at base temperature. For both compounds the function

$$\nu_i(T) = \nu_i(0)(1 - (T/T_c)^\alpha)^\beta \quad (2)$$

was used to fit the temperature dependences of the precession frequencies  $\nu_i(T)$ , where  $T_c$  is the appropriate ordering temperature,  $\alpha$  describes the temperature dependence as  $T \rightarrow 0$ , and  $\beta$  is the critical parameter describing the sublattice magnetization close to  $T_c$  [25].

### 3. $\mu\text{SR}$ measurements on $\text{LaTiO}_3$

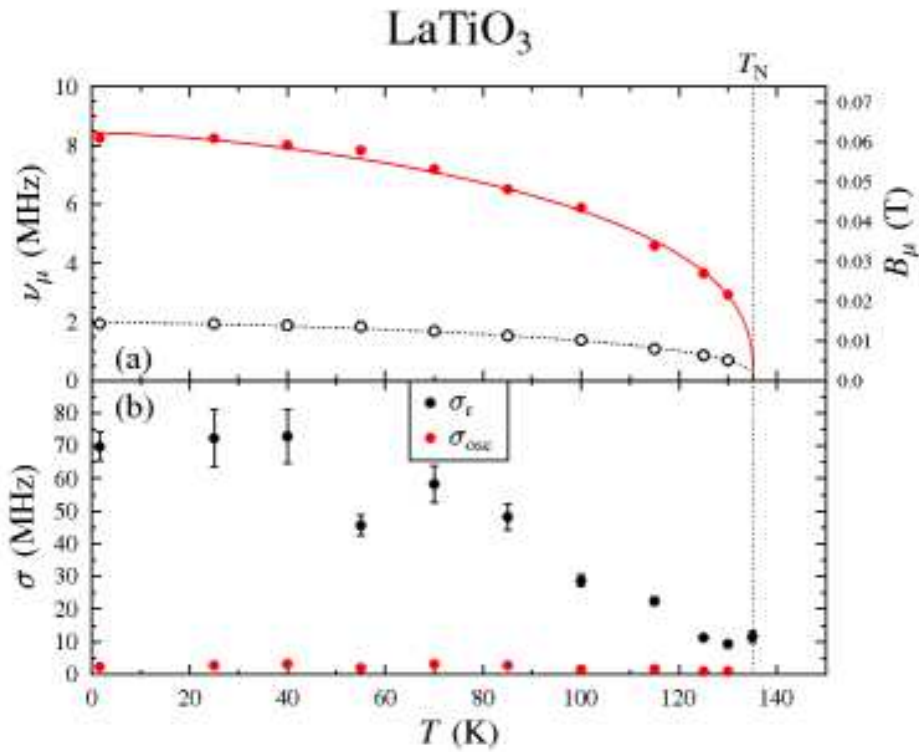


**Figure 3.** Parameters extracted from the raw  $\mu\text{SR}$  data on  $\text{LaTiO}_3$  using Equation 1: (a) Precession frequencies  $\nu_1$  and  $\nu_2$ , together with the equivalent magnetic field. (b) Gaussian relaxation rate and linewidth,  $\sigma_r$  and  $\sigma_{\text{osc}}$ . Fitted lines in (a) are to Equation 2 with the parameters discussed in the text.

Raw data recorded on  $\text{LaTiO}_3$  are shown in Figure 2(a). The high temperature

data are well described by a single exponential relaxation consistent with fast fluctuating electronic moments in the paramagnetic phase. Muon precession is clearly evident in the ordered phase. The fits shown in Figure 2(a) were to equation 1. The ratio  $\nu_2/\nu_1$  was set to 0.234 from the base temperature data. We see that the precession is rapidly damped in the ordered phase since the linewidth is comparable to the precession frequencies. The parameters obtained from fitting Equation 1 to the asymmetry data, applying these constraints, are shown in Figure 3.

Both precession frequencies shown in Figure 3(a) are well defined up to  $T_N$ , although it was not possible to resolve a precession signal in the 135 K dataset even though the fast relaxing component was still evident at this temperature, whereas  $A(t)$  for  $T \geq 140$  K took the simple exponential form expected for a fast-fluctuating paramagnetic phase. The values of  $\nu_1$  were fitted to Equation 2 with  $\alpha = 1.5$ , leading to the parameters  $\nu_1(0) = 8.4(1)$  MHz,  $\beta = 0.37(3)$ , and  $T_N = 135(1)$  K. This value of  $T_N$  is consistent with the value found by Zhou and Goodenough [17], and it is conceivable that other magnetic studies may have been strongly affected by small regions with slightly different oxygen stoichiometry, giving the appearance of a slightly higher  $T_N$ . The linewidth of the oscillating components,  $\sigma_{osc}$ , is close to being temperature independent,  $\sim 2$  MHz. The Gaussian relaxation rate  $\sigma_r$  is significantly larger than either of the precession frequencies, and roughly scales with the precession frequencies, suggesting that muons are stopping at sites with very large local fields, probably sitting along the magnetic moment direction of nearby  $Ti^{3+}$  ions.

#### 4. $\mu$ SR measurements on YTiO<sub>3</sub>

Asymmetry spectra recorded on YTiO<sub>3</sub> are shown in Figure 2(b). Again, the high temperature data are well described by a single exponentially relaxing component, as is typical for paramagnets. Below  $T_C \sim 27$  K two muon precession frequencies are again observed, consistent with long range magnetic order developing below this temperature. Preliminary fitting showed that the amplitude of each component of Equation 1 was essentially temperature independent below  $T_C$ , with  $(P_f + P_r)/P_{osc} \simeq 2$ , and well defined. The ratio  $\nu_2/\nu_1$  was set to the ratio at base temperature, 0.28. The fits to the data shown in Figure 2(b) are to Equation 1 with the parameters shown in Figure 4.

The two precession frequencies shown in Figure 4(a) remain in proportion for all temperatures below  $T_C = 27$  K. Unlike the situation in LaTiO<sub>3</sub> however, we see that the fast-relaxing Gaussian component has a rate  $\sigma_r$  which follows a similar power law to the precession frequencies. In YTiO<sub>3</sub> the values of  $\nu_1$  and  $\sigma_r$  determined independently in the analysis of the asymmetry data were found to be proportional to one another, in agreement with the model of muon sites with very large local fields suggested above, so both were fitted to Equation 2 in parallel, fixing  $\alpha = 1.5$ , leading to the parameters  $\nu_1(0) = 41(1)$  MHz,  $\sigma_r(0) = 103(2)$  MHz,  $\beta = 0.39(4)$ , and  $T_C = 26.0(4)$  K. The linewidth of the oscillating components is  $\sim 10$  MHz at low temperature, falling slightly towards the transition.

#### 5. Dipole field calculations

The magnetic structures of LaTiO<sub>3</sub> and YTiO<sub>3</sub> have previously been determined using neutron scattering [6, 7, 8], although there remained some uncertainty over

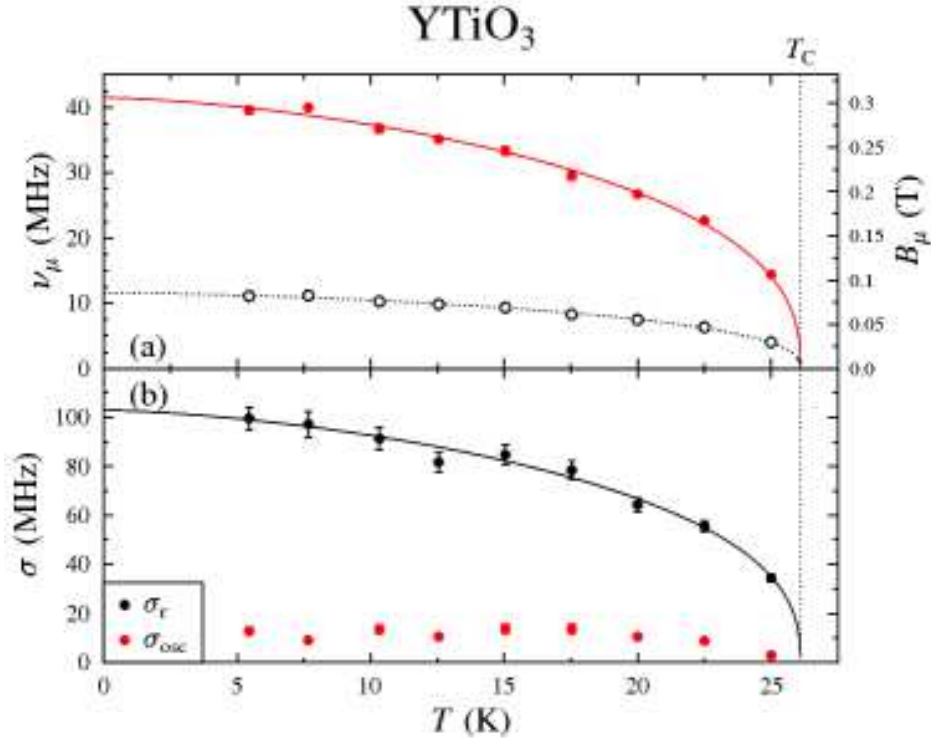


**Figure 4.** Parameters extracted from the raw  $\mu\text{SR}$  data on  $\text{YTiO}_3$  using Equation 1 as discussed in the text. (a) Precession frequencies  $\nu_1$  and  $\nu_2$ , together with the equivalent magnetic field. (b) Gaussian relaxation rate and linewidth,  $\sigma$  and  $\sigma_{\text{osc}}$ . Fitted lines are to Equation 2 with the parameters discussed in the text.

the orientation of the magnetic moments in  $\text{LaTiO}_3$  [7]. These magnetic structures can be compared with the  $\mu\text{SR}$  data by calculating the dipolar fields:

$$B_{\text{dip}}(\mathbf{r}_\mu) = \frac{\mu_0}{4\pi} \sum_i \frac{3(\mu_i \cdot \hat{\mathbf{n}}_i)\hat{\mathbf{n}}_i - \mu_i}{|\mathbf{r}_\mu - \mathbf{r}_i|^3}, \quad (3)$$

where  $\mathbf{r}_\mu$  is the position of the muon,  $\mu_i$  is the ordered magnetic moment of the  $i$ th Ti ion and  $\hat{\mathbf{n}}_i (= (\mathbf{r}_\mu \mathbf{r}_i) / |\mathbf{r}_\mu - \mathbf{r}_i|)$  is the unit vector from the Ti ion at site  $\mathbf{r}_i$  to the muon for points within the unit cell. Contributions from of order  $10^4$  unit cells were considered. Of course, this method neglects the hyperfine contact field, the Lorentz field and the demagnetizing field, although the latter two are zero for antiferromagnets and the contribution of the former to the magnetic field experienced at muon stopping sites,  $\sim 1 \text{ \AA}$  from  $\text{O}^{2-}$  ions, is generally small. The details specific to each compound will be discussed in sections 5.1 and 5.2 below.

Such dipole field calculations have been compared to  $\mu\text{SR}$  data in other perovskite compounds. Some of the more thoroughly studied materials have been the rare earth orthoferrites,  $R\text{FeO}_3$ . The  $R = \text{Sm, Eu, Dy, Ho, Y, and Er}$  variants were studied by Holzschuh *et al.* [26] and they found that the stable muon site common to all of

these compounds was on the mirror plane at  $z = 1/4(3/4)$ , this being the rare earth–oxygen layer, either about 1 or 1.6 Å from the nearest oxygen ion, as would be expected for the  $(\text{OH})^-$  analog,  $(\text{O}\mu)^-$ . This study was followed by others taking a slightly different approach to finding the muon sites [27, 28], and these found further plausible sites, albeit apparently metastable ones, neighbouring the rare earth–oxygen layers. Results of these studies have also been applied to orthorhombic nickelates, without precession frequencies to test the hypothesis, but the approach was consistent with phase separation occurring within magnetically inequivalent layers [29]. The most immediately relevant example within the literature is  $\text{LaMnO}_3$  [30], for which a detailed study showed that the two observed precession frequencies corresponded to two structurally inequivalent muon sites, the lower frequency one within the rare earth–oxygen mirror plane and the higher frequency one at an interstitial site within the Mn–O plane. The latter site requires a significant contribution from the contact fields due to the neighbouring oxygen ions, which the dipole field calculations presented here do not consider.

### 5.1. $\text{LaTiO}_3$

Dipole field calculations were carried out for the  $G$ -type magnetic structure reported in Ref. [6] and shown in Figure 1(a), assuming the magnetic moments ( $\mu = 0.57 \mu_B$ ) are aligned along the  $a$ -axis [7]. Calculations were also carried out assuming alignment along the  $c$ -axis as this possibility had previously been favoured and neutron measurements did not clearly exclude it [6, 7]. The results are periodic in the  $c$ -axis by half the orthorhombic  $c$ -axis lattice constant. We would expect the muon sites to lie within the  $z = 1/4$  plane, as they do in  $\text{LaMnO}_3$  [30]. If the moments are along the  $c$ -axis, the only contours corresponding to both observed precession frequencies are very closely spaced at points around 0.75 Å from the oxygen ion centres within the plane. For moments aligned along the  $a$ -axis the calculations give results much more similar to those in  $\text{LaMnO}_3$ . Since we expect the O– $\mu$  bond to be around 1 Å, this moment orientation seems far more consistent with the observed precession frequencies. The other possibility is that the muon sites lie within the Ti–O layer. This is far more consistent with moment alignment along the  $c$ -axis, since suitable field values are found at sites between oxygen ions. It is more difficult to make precise assignment of muon sites in this case because the field contours are far more closely spaced. While there remains some ambiguity, observing well separated field contours corresponding to previously identified muon sites for similar materials, and apparently equally numbers of plausible muon sites for each frequency, in agreement with the experimental amplitudes, is strong evidence that the moments are aligned along  $a$  rather than  $c$ , something neutron results have not been able to demonstrate with more certainty [7].

### 5.2. $\text{YTiO}_3$

Dipole field calculations were carried out for the ferromagnetic structure reported in Ref. [8], with moment values of  $(0.106, 0.0608, 0.7034) \mu_B$  along the principal axes of the pseudocubic unit cell  $(a, b, c)$ , and depicted in Figure 1(b). The calculations show that the magnetic fields for this largely ferromagnetic structure are much greater than those in the antiferromagnetic structure of  $\text{LaTiO}_3$ . As in  $\text{LaTiO}_3$  the lower frequency component in the signal is consistent with sites within the A–O plane ( $z = 1/4$ ), but



there are no sites within this layer that would correspond to the higher frequency observed. The higher frequency component appears consistent with a smaller number of sites between oxygen ions near to or in the  $z = 1/2$  layer, but rather closer to the  $\text{Ti}^{3+}$  ion positions. There are also plausible sites corresponding to the lower frequency within this layer. Because of the small magnetic moments along the  $a$  and  $b$ -axes the contours are more distorted than those calculated for  $\text{LaTiO}_3$ . Considering the variation of these distortions along the  $c$ -axis leads to a structure not dissimilar to a helically ordered magnet, for these small components. This could also lead to structurally equivalent sites with much higher local fields but significant magnetic inequivalencies, leading to the fast-relaxing component,  $P_r$ , of the observed asymmetry.

## 6. Discussion

The  $\mu\text{SR}$  results clearly demonstrate intrinsic magnetic order below the expected ordering temperatures in both samples. We are also able to follow the temperature dependence of the (sub)lattice magnetization and show that the behaviour is essentially conventional. The values of  $\beta$  derived from Equation 2 describe the behaviour close to the transition temperature. The values of  $\beta = 0.37$  ( $\text{LaTiO}_3$ ) and  $\beta = 0.39$  ( $\text{YTiO}_3$ ) are significantly below the mean field expectation of 0.5 and lie within the range 0.3-0.4 consistent with 3D critical fluctuations (e.g. 0.346 (3D XY) or 0.369 (3D Heisenberg)) [31]. This is reasonable in the context of the relatively isotropic nature of the exchange interactions in these compounds.

In the context of the dipole field calculations described in Section 5 and the previous literature, the sites obtained for the two compounds considered here seem entirely plausible. For both compounds we find a site corresponding to the lower precession frequency in the A–O layer, as in  $\text{LaMnO}_3$ , but the origin of the higher frequency component is almost certainly different in the two cases. In  $\text{LaTiO}_3$  the higher frequency sites also appear to be in the rare earth–oxygen layer, and this fits with the equal amplitudes of the two components observed in the  $\mu\text{SR}$  signal. Sites near the Ti–O planes seem unlikely on the basis of the calculations. In  $\text{YTiO}_3$  the higher frequency component cannot be in the Y–O plane if the hyperfine coupling is negligible. A more plausible assignment corresponds to sites lying between two oxygen ions and relatively close to the Ti ions, which would explain the high precession frequency, the relatively small amplitude (since the site would probably be less electrostatically favourable), and also the large initial phase offset, consistent with a stronger coupling to the antiferromagnetically coupled moments in the  $ab$ -plane. Lower frequency sites could also occur in the Ti–O layers. In both compounds a full site determination would require measurements on single crystals and in applied fields, as was done for the rare earth orthoferrites [26, 27, 28] and  $\text{LaMnO}_3$  [30].

In magnetically ordered polycrystalline samples we would expect the relaxing component to account for around one third of the relaxing asymmetry, owing to the polycrystalline averaging of the effects of the magnetic fields parallel and perpendicular to the muon spin direction. The situation in these materials is not this straightforward. The fast initial relaxation  $\sigma_r$  is most likely to originate from large magnetic fields at muon stopping sites which are slightly magnetically inequivalent. The dipole field calculations suggest that both compounds have plausible stopping sites close to the magnetic moment directions of nearby  $\text{Ti}^{3+}$  ions, where a small range of muon stopping positions would give sufficiently different magnetic fields to lead to this fast relaxing component. Because of this rapid depolarization we are unable to

distinguish the relaxation due to fields parallel to the muon spin direction and the amplitude  $P_r$  is likely to include the longitudinal relaxing component usually observed in polycrystalline magnets as well as the contribution from muons stopping at sites with very high local fields.

The results presented in this paper are in excellent agreement with previous reports of the magnetic properties of both  $\text{LaTiO}_3$  and  $\text{YTiO}_3$  obtained using neutron diffraction [6, 8]. This confirmation is worthwhile given the history of sample dependent results and the difficulty of controlling the oxidation state precisely [9, 17]. Comparison between the precession frequencies observed in  $\text{LaTiO}_3$  and dipole field calculations strongly favours moment alignment along the  $a$ -axis rather than the  $c$ -axis, an issue powder neutron diffraction has difficulty resolving [7]. Using a microscopic probe gives an independent means of testing the previous results from bulk probes; our results confirm that despite the complexities of the underlying orbital physics, both compounds behave magnetically as bulk, three-dimensional magnets. We are also able to test the ability of dipole field calculations to reproduce the magnetic field distributions within oxide materials. This is successful for these compounds, where the similarity of both the structure and the muon sites nevertheless yields different internal fields due to the significantly different magnetic structures.

## 7. Acknowledgements

Part of this work was carried out at the Swiss Muon Source, Paul Scherrer Institute, Villigen, Switzerland. We thank Alex Amato for technical assistance. This research project has been supported by the EPSRC and by the European Commission under the 6th Framework Programme through the Key Action: Strengthening the European Research Area, Research Infrastructures, Contract no R113-CT-2003-505925. TL acknowledges support from the Royal Commission for the Exhibition of 1851.

## References

- [1] Cox PD *Transition Metal Oxides: an introduction to their electronic structure and properties*, (Clarendon Press, Oxford, 1992)
- [2] Komarek AC, Roth H, Cwik M, Stein W-D, Baier J, Kriener M, Bourée F, Lorenz T, and Braden M 2007 *Phys. Rev. B* **75** 224402
- [3] Solovyev IV 2006 *Phys. Rev. B* **74** 054412
- [4] Mochizuki M and Imada M 2004 *New J. Phys.* **6** 154
- [5] Tokura Y and Nagaosa N 2000 *Science* **288** 462
- [6] Keimer B, Casa D, Ivanov A, Lynn JW, Zimmermann Mv, Hill JP, Gibbs D, Taguchi Y, and Tokura Y 2000 *Phys. Rev. Lett.* **85** 3946
- [7] Cwik M, Lorenz T, Baier J, Müller R, André G, Bourée F, Lichtenberg F, Freimuth A, Schmitz R, Müller-Hartmann E, and Braden M 2003 *Phys. Rev. B* **68** 060401
- [8] Ulrich C, Khaliullin G, Okamoto S, Reehuis M, Ivanov A, He H, Taguchi Y, Tokura Y, and Keimer B 2002 *Phys. Rev. Lett.* **89** 167202
- [9] Ulrich C, Gössling A, Grüniger M, Guennou M, Roth H, Cwik M, Lorenz T, Khaliullin G, and Keimer B 2006 *Phys. Rev. Lett.* **97** 157401
- [10] MacLean DA, Ng H-N, and Greedan JE 1979 *J. Solid State Chem.* **30** 35
- [11] Haverkort MW, Hu Z, Tanaka A, Ghiringhelli G, Roth H, Cwik M, Lorenz T, Schüßler-Langeheine C, Streltsov SV, Mylnikova AS, Anisimov VI, de Nadai C, Brookes NB, Hsieh HH, Lin H-J, Chen CT, Mizokawa T, Taguchi Y, Tokura Y, Khomskii DI, and Tjeng LH 2005 *Phys. Rev. Lett.* **94** 056401
- [12] Hemberger J, Krug von Nidda H-A, Fritsch V, Deisenhofer J, Lobina S, Rudolf T, Lunkenheimer P, Lichtenberg F, Loidl A, Bruns D, and Büchner B 2003 *Phys. Rev. Lett.* **91** 066403
- [13] Akimitsu J, Ichikawa H, Eguchi N, Miyano T, Nishi M, and Kakurai K 2001 *J. Phys. Soc. Japan* **70** 3475

- [14] Iga F, Tsubota M, Sawada M, Huang HB, Kura S, Takemura M, Yaji K, Nagira M, Kimura A, Jo T, Takabatake T, Namatame H, and Taniguchi M 2004 *Phys. Rev. Lett.* **93** 257207; 2006 *Phys. Rev. Lett.* **97** 139901(E)
- [15] Khaliullin G and Maekawa S 2000 *Phys. Rev. Lett.* **85** 3950
- [16] Kiyama T and Itoh M 2003 *Phys. Rev. Lett.* **91** 167202
- [17] Zhou HD and Goodenough JB 2006 *Phys. Rev. B* **71** 184431
- [18] Mochizuki M and Imada M 2003 *Phys. Rev. Lett.* **91** 167203
- [19] Pavarini E, Biermann S, Poteryaev A, Lichtenstein AI, Georges A, and Andersen OK 2004 *Phys. Rev. Lett.* **92** 176403
- [20] Schmitz R, Entin-Wohlman O, Aharony A, Harris AB, and Müller-Hartmann E 2005 *Phys. Rev. B* **71** 144412; 2007 *Phys. Rev. B* **76** 059901(E)
- [21] Khaliullin G and Okamoto S 2002 *Phys. Rev. Lett.* **89** 167201
- [22] Khaliullin G and Okamoto S 2003 *Phys. Rev. B* **68** 205109
- [23] Itoh M, Tsuchiya M, Tanaka H, and Motoya K 1999 *J. Phys. Soc. Japan* **68** 2783
- [24] Blundell SJ 1999 *Contemp. Phys.* **40** 175
- [25] Blundell SJ *Magnetism in Condensed Matter Physics*, (OUP, Oxford, 2001).
- [26] Holzschuh E, Denison AB, Kündig W, Meier PF, and Patterson BD 1983 *Phys. Rev. B* **27** 5294
- [27] Boekema C, Lichti RL, and Rüegg KJ 1984 *Phys. Rev. B* **30** 6766
- [28] Lin TK, Lichti L, Boekema C, and Denison AB 1986 *Hyp. Int.* **31** 475
- [29] García-Muñoz JL, Lacorre P, and Cywinski R 1995 *Phys. Rev. B* **51** 15197
- [30] Cestelli Guidi M, Allodi G, De Renzi R, Guidi G, Hennion M, Pinsard L, and Amato A 2001 *Phys. Rev. B* **64** 064414
- [31] Pelissetto A and Vicari E 2002 *Phys. Rep.* **368** 549